Khaled MILOUDI[1,2], Hocine MOULAI[1], Hakim AZIZI[1,3]

LCDEP Laboratory, Electrical Engineering Faculty, University of Science and Technology Houari Boumediene, Algiers, Algeria (1)
University Echahid Hamma Lakhdar – El-oued – BP 789 El-oued, Algeria (2)
University Ziane Achour of Djelfa, PO 3117, Algeria (3)
ORCID: 1. 0000-0002-5106-2821

doi:10.15199/48.2023.10.174

Modeling and Numerical Simulation of Eddy Current Sensors for Electromagnetic Characterization of Fluids

Abstract*. This work aims to model a device enabling a useful and accurate electromagnetic characterization of fluids. The device developed is based on a non destructive testing (NDT) control technique evolving the eddy currents induced in the fluid to be characterized. The finite element method was used in the modeling to determine the conductivity of the fluid from the induced eddy current. In addition, an experimental device has been built. It consists of an absolute probe where the fluid control is made by determining its electrical conductivity by measuring the variations of the fluid impedance as a function of the applied voltage frequency. Good agreements are found between modeling results and experimental measurements. An inverse model that converges after only 7 iterations has been also proposed for the determination of the conductivity of fluids by the use of theoretical and experimental measurements.*

Streszczenie. *Niniejsza praca ma na celu zamodelowanie urządzenia umożliwiającego użyteczną i dokładną charakterystykę elektromagnetyczną płynów. Opracowane urządzenie opiera się na technice kontroli badań nieniszczących (NDT), która rozwija prądy wirowe indukowane w scharakteryzowanym płynie. W modelowaniu wykorzystano metodę elementów skończonych do wyznaczenia przewodności płynu z indukowanych prądów wirowych. Ponadto zbudowano eksperymentalne urządzenie. Składa się z sondy absolutnej, w której kontrola płynu odbywa się poprzez określenie jego przewodności elektrycznej poprzez pomiar zmian impedancji płynu w funkcji przyłożonej częstotliwości napięcia. Stwierdzono dobrą zgodność między wynikami modelowania a pomiarami eksperymentalnymi. Zaproponowano również model odwrotny, który zbiega się już po 7 iteracjach, do wyznaczania przewodnictwa płynów za pomocą pomiarów teoretycznych i eksperymentalnych. (****Modelowanie i symulacja numeryczna czujników prądów wirowych do charakterystyki elektromagnetycznej płynów****)*

Keywords: NDT, Inductive sensor, Absolute probe, Finite elements, Electromagnetic, Inverse problem.
Słowa kluczowe: NDT, Czujnik indukcyjny, Sonda absolutna, Elementy skończone, Elektromagnetyczne, Problem odwrotny.

Introduction

The electromagnetic characterization of fluids is a process to be implemented to determine and monitor the concentration of salts in water. It is used in many areas of industrial and environmental analysis [1-3]. Whether cleaning dairy filling pipes, protecting cooling systems in power plants [4, 5] and recently controlling the electrolyte solution for green hydrogen production [6, 7], the correct operations always depend on the conductivity value.

There are two main techniques to measure electrical conductivity of fluids [8, 9]: the most widely used is the classical technique (measurement by conduction) which consists of two electrodes and a plunger which brings them together. The two electrodes are subjected to a constant alternating voltage and the measurement signal is the current flowing through the solution to be characterized.

On the other hand, in induction measuring cells, the electrodes are replaced by two coils. One of the coils crossed by an alternating current produces a magnetic field in its environment; it is used for excitation according to the Maxwell-Ampere principle. This coil is inserted into the solution to be characterized. The magnetic field of the coil thus induces in the medium to be characterized an eddy current, which in turn produces a magnetic field [10, 11]. This magnetic field thus induces in the second coil (receiver) an alternating voltage according to the Maxwell-Faraday principle which is the image of the primary current and of the medium traversed by the induced field. This voltage depends directly on the current which circulates in the solution, therefore on its conductivity.

The task of this investigation consists of determining the physical characteristics (especially the electrical conductivity) of a fluid by analyzing the response of an eddy current sensor. The work includes a numerical simulation section which will be validated by experimental measurements.

In this context, an electromagnetic inspection device has been dimensioned and several types of fluid with different conductivities are characterized. The achieved prototype was tested in order to validate the theoretical model implemented under MATLAB and solved by the finite element method.

Problem modeling

The equations governing the general time varying fields include magnetic and conducting fluids can be derived from the following Maxwell equations [12- 15]:

(1) $\nabla . E = \rho / \varepsilon$ Maxwell-Gauss equation:

(2) : $\nabla . B = 0$ Magnetic flux conservation equation

(3) $\nabla\times B = \mu (J + \delta D / \delta t)$ Maxwell-Ampere equation

(4) $\nabla\times E = - \delta B / \delta t$ Maxwell-Faraday equation

Where induction, magnetic and electric fields are linked respectively by the following relations:

(5) $B = \mu H$

(6) $D= \varepsilon E$

In a conductive medium, we also have Ohm's law:

(7) $J = \sigma E.$

Where ρ represents the volumic density of the electric charges (C/m^3), B the magnetic induction (Wb/m^2), H the magnetic field (A / m), D the electric induction (C/m^2), E the electric field (V/m) and J the conduction current density (A/m^2)

μ, ε and σ represent respectively the permeability, the permittivity and the conductivity of the medium (S/m).

As the magnetic induction is of null divergence, a potential magnetic vector A can be introduced such as:

$$B=\nabla\times A \quad (8)$$

The field E can be expressed according to the magnetic potential vector A and the electric potential such as:

(9) $E= - \partial A/\partial t - \nabla V$

The local form of the Ampere's theorem and the conservation law are written as follows [16-18].

(10) $\nabla^2 A + K^2 = -\mu J$

(11) $K^2 = -j\omega\mu\,(\sigma + j\omega\varepsilon)$

Where ω is the angular frequency of the excitation current (rad/s), H the magnetic field (A/m) and σ the conductivity of the medium (S/m). A represents the magnetic potential vector, μ the magnetic permeability, J the excitation current density and ε the dielectric constant. The eddy current problem can be described mathematically by an equation in terms of the magnetic potential vector A [19-21].

The Khalestki algorithm is applied to solve this kind of equations by taking advantage of the symmetry and bandwidth [22]. This enabled to determine A at the nodes of the finite element mesh. Moreover, from A, other quantities can be calculated such as flux densities and coil impedances [23, 24].

Impedance calculation

After determining the magnetic potential vector A on all the nodes of the different regions of the device to be studied, the impedance of the coil can be calculated by two different commonly used approaches: the direct method and the energy method.

The direct method

The impedance of a single turn of the coil (probe) crossed by an alternating current I_0 is given by :

(12) $Z = \frac{V}{I_0}$

Where V is the voltage induced in the coil, expressed as a function of the electric field intensity E as:

(13) $V = -\int E dl$

From equation (9), we have:

(14) $E = -\frac{\partial A}{\partial t} - gradV$

In harmonic regime:

(15) $\frac{\partial}{\partial t} = j\omega$

And one obtains then:

(16) $E = -j\omega A - gradV$

The induced voltage is independent on the scalar potential (grad V=0). Thus, by replacing (16) in (13), one obtains:

(17) $V = jw \int A.dl$

From equation (12), the coil impedance becomes:

(18) $Z = \frac{jw}{I_0} \int A.dl$

From where for a single turn of radius r, we will have:

(19) $Z = j\frac{2.\pi.w.r.A}{I_0}$

The sensor impedance is constituted of two parts: A real part which is the resistance and an imaginary part which is the reactance.

(20) $Z = R + j.X$

By calculating the magnetic potential vector at the center of each turn A_i, and if N_s is the total number of turns and r_i the radius of each turn, the total impedance of all the turns of the coil is given by:

(21) $Z = j\frac{2.\pi.w}{I_0}\sum_{i=1}^{N_s} r_i.A_i$

Finite elements method processing

In order to solve the problem by the finite element method, we proceed in successive stages as depicted on figure 1:

- The physical problem in posed in the form of a differential equation to be satisfied at any point of the domain Ω, with ∂Ω boundary conditions that are necessary and sufficient to the solution to be unique.
- An integral formulation of the differential system is built to be solved with its boundary conditions: This consists in the variational formulation of the problem. The domain Ω is then divided into cells
- One chooses the family of local fields, i.e. at the same time the position of the nodes in the sub domains and the polynomials (or other functions) which define the local field according to the values with the nodes (and eventually derivatives). The mesh completed by this information then becomes an element.
-

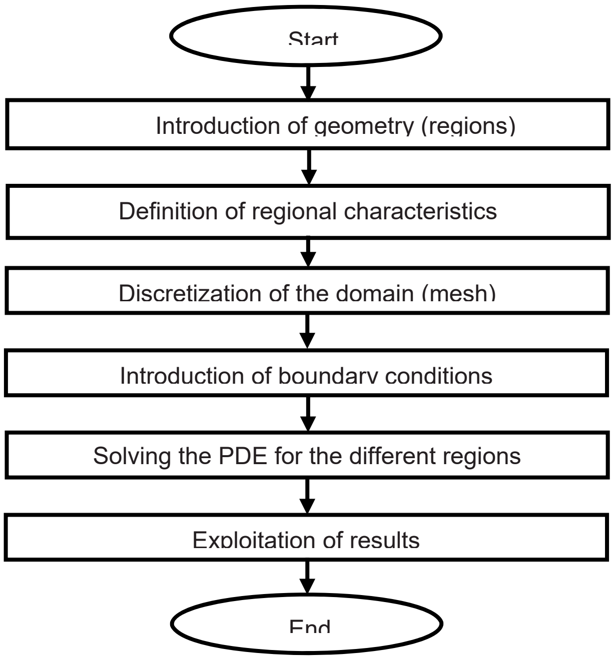

Fig 1. Flowchart used to solve the problem by the finite elements method

- The problem is then reduced to a discrete problem. Indeed, any approximated solution is completely determined by the values at the nodes of the elements. It is therefore sufficient to find the values to be assigned to the nodes to describe an approximate solution. A discrete problem is then solved.
- Phase of post processing where one builds the approximate solution starting from the values found with the nodes and to deduce other quantities.
- The solution is then visualized to judge its digital quality and whether it satisfies the specifications criteria: This is the exploitation of the results.

Simulations and discussions

The experimental test bench is depicted on figure 2. It is mainly composed of the solution container, the excitation coil, the LCR meter (GW INSTEK: LCR-8110G, 20 Hz - 10MHz), the measurement coil and the PC. The characteristics of the measurement coil are detailed on table 1.

Table 1: Geometric characteristics of the sensor

The coil	
Inner radius (Ri)	4 mm
Outer radius (Ro)	13.6 mm
Length (L)	11.2 mm
Number of vertical turns	14
Number of horizontal turns	12
Number of turns (N)	168
Winding wire radius	0.3 mm

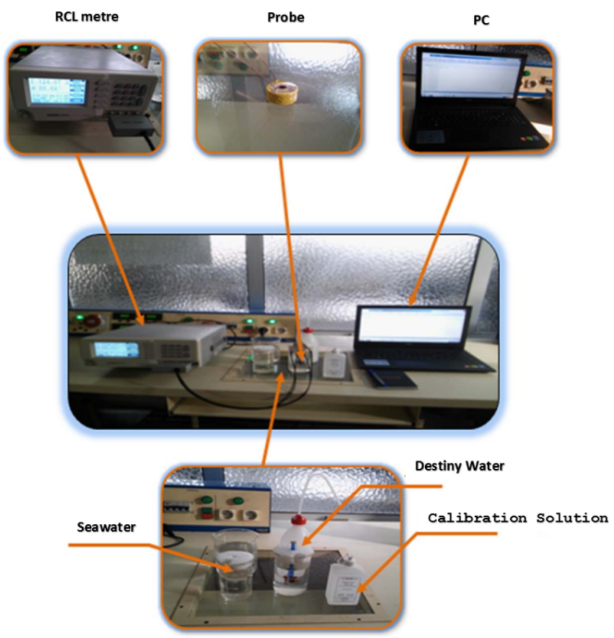

Fige 2: Experimental test bench

Influence of geometric and physical parameters on the measurement efficiency:

Evaluating the variation of the impedance as a function of conductivity

In figures 3.a and 3.b, three fluids (seawater, NaCl, HCl) are tested, where the position of the coil and the volume of the fluid are fixed. Then, the variation of the corresponding impedance of each fluid is calculated versus frequency. It is shown that the more the conductivity increases the more the real part of the impedance becomes high. This can be justified by the distribution of eddy currents reaction, where they increase for conductive fluids. This distribution of current makes a greater flow in the fluid and therefore a greater resistance.

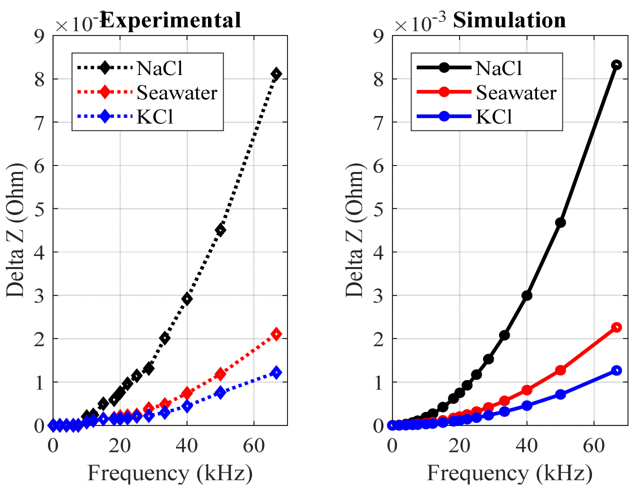

Fig/ 3: Variations of impedance as a function of frequency for different fluids.

Variations of the impedance as a function of the solution volume

On figure 4, one type of fluid has been investigated (the seawater), and the position of the coil has been fixed at the center of the solution. Then, the fluid volume is varied between 100ml and 1.2 litre, and the variation of the corresponding impedance is determined.

The variation of impedance as a function of frequency for different volumes shows an exponential variation (the more the frequency is increased, the more the delta Z increases).

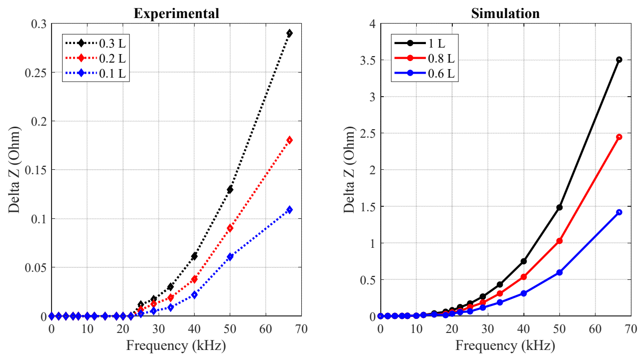

Fig. 4. Impedance variations versus frequency for different volumes

Variations of the impedance as a function of the coil position

The position of the coil in the fluid is an important factor that must be taken into account when performing measurements. In figure 5, the variations of the impedance of seawater as a function of the depth of the coil in the fluid are presented for a fixed volume of 1 liter. According to figures 5a and b, it was found that the optimal position is located at the center of the fluid container. Indeed, in this position, the magnetic coupling is maximal between the sensor and the fluid (50% L). So, from this middle position the measurements are performed.

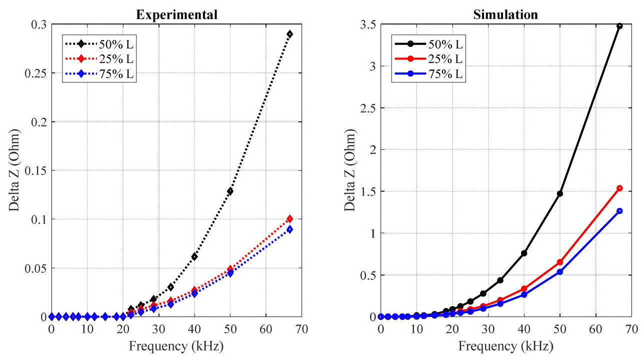

Fig. 5: Variations of the impedance versus frequency for different positions of the coil.

Reverse problem treatment

In general, direct models are rarely invertible. The solution consists in placing the direct model of the device in a feedback loop. The output of the direct model is then compared to the acquisitions made, and the error thus observed is proposed as input to an optimization algorithm which consequently modifies the estimations of the expected characteristics. At each iteration, this modification aims to minimize the error obtained. The inversion is assumed to be correct and the process is stopped when this error becomes less than a limit value fixed as a criterion for stopping the iterations. The most commonly used algorithms are based on the calculation of the gradient of the error criterion [25, 26]. The used diagram of the inversion process is given in Figure 6.

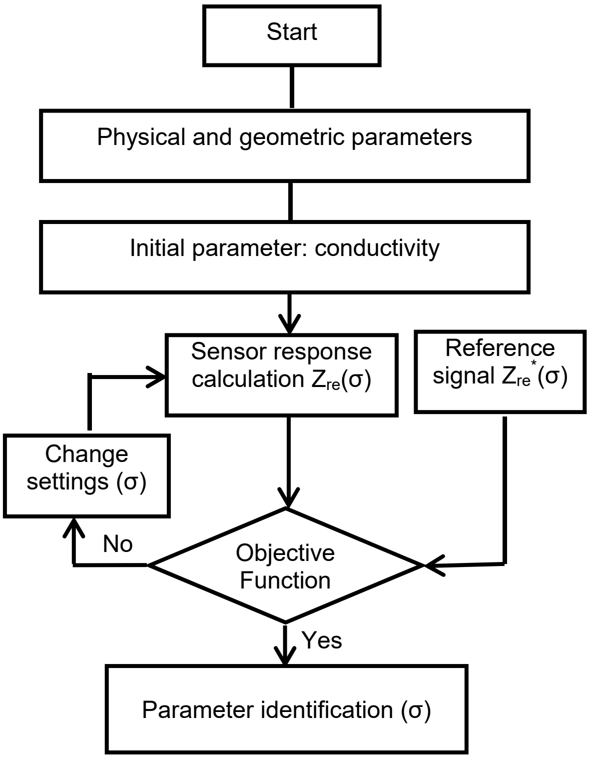

Fig. 6. The flowchart of the reversal procedure

The objective function to be minimized is stated as follows:

$$S = Z_{re} - Z_{re}^{*} \quad (22)$$

where Zre* is the real part of the reference impedance

Validation of the approach

In the following, 300ml at a 1mol/l of KCl calibration solution was prepared from a known conductivity of 1.28 Siemens / m. Then, the variations of resistance are measured as a function of frequency, and the obtained results are illustrated on figure 7.

The initial value used for the inversion consists of a conductivity of 0.5 S / m. It has been found that the conductivity reaches the reference value after 7 iterations. One observes the convergence of the inversion program towards the optimal solution, which once again validates the direct calculation program.

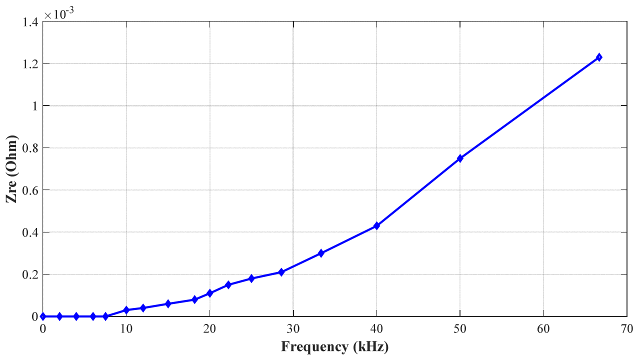

Fig/ 7. KCl reference signal used for the numerical validation of the approach.

Conclusions

An electromagnetic sensor is achieved to be used in the field of nondestructive detection and evaluation of the physical characteristics of fluids. The detection method is based on the behavior of eddy currents in these fluids. Thus, the formulation of the electromagnetic problem is carried out from Maxwell's equations to arrive at the partial differential equation depicting the behavior of the phenomenon to be studied. Partial differential equations are solved in the case of an absolute sensor by the finite element method with axisymmetric assumptions. The results analysis shows the influence of the physical and geometric characteristics (volume and position of the coil and fluid conductivity) on the impedance of the sensor.

At the end, we conclude that:

The impedance of the fluid sensor increases with the increase in volume of fluid up to a certain level where it becomes constant (saturation of the coil).

The best position of the coil is in the middle of the fluid, which corresponds to a maximum magnetic coupling.

A well correlation between the fluid conductivity and the impedance of the sensor-fluid is found. The influence of this physical characteristic on the measurement of the impedance is more remarkable in the real part of the impedance than in its imaginary part. Thus, an efficient assessment of the electrical conductivity of a fluid is obtained thanks to the variations of the real part of the impedance as a function of frequency.

An iterative inversion algorithm has been developed and used successfully. After only 7 iterations, it convergences to the results provided by the direct model whose signals are considered as reference. The developed technique was validated on the three samples of fluids where good agreement is found between the simulation results and the experimental measurements.

***Authors**: Khaled Miloudi, University Echahid Hamma Lakhdar – El-oued – BP 789 El-oued, Algeria; Email: miloudi-khaled@univ-eloued.dz; Prof. Hocine Moulai, University of Science and technology Houari Boumediene, Bab Ezzouar, Algiers 16025 Algeria; Email: hmoulai@usthb.dz; Dr Hakim Azizi, University Ziane Achour of Djelfa, PO 3117, Algeria; Email: azizihakimbilal@yahoo.fr.*

REFERENCES

[1] Vincent Guihard, Cédric Patapy, Julien Sanahuja, Jean-Paul Balayssac, Frédéric Taillade, and Barthélémy Steck, Effective medium theories in electromagnetism for the prediction of water content in cement pastes, International Journal of Engineering Science, Volume 150, May 2020, 103273

[2] Xavier Dérobert, Géraldine Villain, Effect of water and chloride contents and carbonation on the electromagnetic characterization of concretes on the GPR frequency band through designs of experiment, NDT & E International, Volume 92, December 2017, Pages 187-198

[3] AnaMarta Paz, Nádia Castanheira, Mohammad Farzamian, Ma riaCatarina Paz, MariaConceição Gonçalves, Fernando A. Monteiro Santos, John Triantafilis, Prediction of soil salinity and sodicity using electromagnetic conductivity imaging, Geoderma, Volume 361, 1 March 2020, 114086

[4] R.P. Singh, S.E. Zorrilla, S.K. Vidyarthi, R. Cocker, K. Cronin, Dairy Plant Design, Construction and Operation, Encyclopedia of Dairy Sciences (Third edition) 2022, Pages 239-252

[5] S.A. Rankin, R.L. Bradley, G. Miller, K.B. Mildenhall, *A 100-Year Review:* A century of dairy processing advancements—Pasteurization, cleaning and sanitation, and sanitary equipment design, Journal of Dairy Science, Volume 100, Issue 12, December 2017, Pages 9903-9915

[6] S. Thiel, V. Seiß and M. Eichelbaum, Scanning electrochemical microscopy for the characterization of fuel cell components*, 2022 International Workshop on Impedance Spectroscopy (IWIS),* Chemnitz, Germany, 2022, pp. 14-19, doi: 10.1109/IWIS57888.2022.9975128.

[7] [7] Yueyue Du , Zhi Ying , Xiaoyuan Zheng , Binlin Dou , Guomin Cui, Correlating electrochemical biochar oxidation with electrolytes during biochar-assisted water electrolysis for hydrogen production, Fuel, Vol. 339, 2023, 126957
[8] Monjur Mourshed, Huy Quoc Nguyen, Bahman Shabani, Using electrical conductivity to determine particle sedimentation status of carbon-based slurry electrodes in electrochemical energy storage systems, Materials Science for Energy Technologies, Vol. 6 (2023) 290–300
[9] Xuan Guo, Qi Chen, HuaiWei Ni, Electrical conductivity of hydrous silicate melts and aqueous fluids: Measurement and applications, Sci. China Earth Sci. 59, 889–900 (2016). https://doi.org/10.1007/s11430-016-5267-y
[10] Hamid Mehaddene, Hassane Mohellebi, Azouaou Berkache, Eddy Currents Non Destructive Testing and Evaluation of Ferromagnetic Medium, Przegląd Elektrotechniczny, Vol. 95 No 2, 2019, pp.212-216, doi:10.15199/48.2019.02.26
[11] Daniela Gombarska , Milan Smetana, Wavelet based signal analysis of pulsed eddy current signals, Przegląd Elektrotechniczny (Electrical Review), Vol. 87 No 5, 2011, pp. 37-39
[12] Robert Wald, Advanced Classical Electromagnetism, Princeton University Press, 2022.
[13] J. Doumont-Fillon, ‘’ Control non destructif (CND)’’, Techniques de l’ingénieur, R 1400, Mesures mécaniques et dimensionnelles, 1996.
[14] Prabhakar H. Pathak; Robert J. Burkholder, "Maxwell's equations, constitutive relations, wave equation, and polarization, in *Electromagnetic Radiation, Scattering, and Diffraction,* IEEE, 2022, pp.1-51, doi: 10.1002/9781119810544.ch1.
[15] Mc. G. Warren, ‘’ Essais non destructifs, métaux et matériaux’’, édition Eyrolles , paris, 1967.
[16] Wittig, G. and H.-M. Thomas, « Design of a Pulsed Eddy-Current Test Equipment with Digital Signal Analysis, Eddy-Current Characterization of Materials and Structures », ASTM STP 722, George Bimbaum and George Free, Eds, American Society for Testing Materials, 1981.
[17] Mehran Mirzaei, Pavel Ripka , Vaclav Grim, An eddy current speed sensor with a novel configuration of longitudinal and transversal coils, Sensors and Actuators A: Physical, Volume 352, 2023, 114201
[18] Hagemaier D.J. « Eddy current impedance plane analysis ». Materials Evaluation, 41,1982, pp.211-218.
[19] G. Hrkac, T. Schrefl, M. Schabes, A combined vector and scalar potential method for 3D magnetic fields and transient Eddy current effects in recording head coils, Physica B: Condensed Matter, Volume 384, 2006, pp. 253-255
[20] A. Kameari, Three Dimensional Eddy Current Calculation Using Edge Elements for Magnetic Vector Potential, Applied Electromagnetics in Materials, 1989, pp. 225-236
[21] Ward, W.W. and J.C. Moulder, « Low Frequency Pulsed Eddy Currents for Deep Penetration ». Review of Progress in Quantitative Nondestructive Evaluation, Vol. 17. Plenum Press, New York, 1998.
[22] Etienne Guerber, Michel Benoit, Stephan T. Grilli, Clément Buvat, A fully nonlinear implicit model for wave interactions with submerged structures in forced or free motion, Engineering Analysis with Boundary Elements, Volume 36, Issue 7, July 2012, Pages 1151-1163
[23] L. Oukhellou, Paramétrisation et Classification des Signaux en Contrôle Non Destructif, Application à la Reconnaissance des Défauts de Rails par Courants de Foucault, Doctorat Thesis, Paris XI Orsay University, France, 1997.
[24] I. Dufour and D. Placko, An original approach to eddy current problems through a complex electrical image concept, *IEEE Transactions on Magnetics*, vol. 32, no. 2, pp. 348-365, 1996, doi: 10.1109/20.486519.
[25] Konstanty Marek Gawrylczyk, Fawwaz Alkhatib, A posteriori error estimators in finite element method for time and frequency domain, Przegląd Elektrotechniczny, vol 11, 2007, 31316
[26] Zejun Chen, Haiquan Zhao, Bias-compensated Adaptive Filter Algorithm under Minimum Error Entropy Criterion, IFAC-PapersOnLine Volume 52, Issue 24, 2019, Pages 93-97